

A Numerical Model of an Experiment of Iron Corrosion

Daniela Mansutti¹, Giuseppina Colicchio², Marialaura Santarelli³

¹ *Istituto per le Applicazioni del Calcolo (CNR), Roma*
d.mansutti@iac.cnr.it

² *Istituto Nazionale per Studi ed Esperimenti di Architettura Navale, Roma*
g.colicchio@insean.it

³ *Dip. di Ingegneria Chimica, Materiali e Ambiente,*
Università degli Studi "La Sapienza", Roma
marialaura.santarelli@uniroma1.it

Abstract

An improvement of a mathematical model of the galvanic iron corrosion, previously presented by one of the authors, is here proposed. The iron(III)-hydroxide formation is, now, considered in addition to the redox reaction. The PDE system, assembled on the basis of the fundamental holding electro-chemistry laws, is numerically solved by a locally refined FD method. For verification purpose we have assembled an experimental galvanic cell; in the present work, we report two tests cases, with acidic and neutral electrolytical solution, where the computed electric potential compares well with the measured experimental one.

Keywords: Iron, redox reaction, kinetics, PDE, numerical simulation.

1. Introduction.

Recently, corrosion processes have been object of numerical simulations built upon 'ab initio' molecular dynamics (for example [1], [2]) that have the limit of focussing on microscopic details while missing the description of global macroscopic aspects and are extremely time consuming (105 hours cpu time for 10^{-6} sec. physical time).

Interesting descriptions have been developed with an inverse modelling approach, quantitative descriptions of the corroded area elaborated on the bases of electrostatic measurements *in situ* (see, for example, [3] and [4]). The model here assembled provides a Direct Numerical Simulation (DNS) of the iron corrosion process as it can be represented via a galvanic cell with anode made of iron. In particular we propose an extension to the

Received 20/02/2009, in final form 31/07/2009

Published 31/07/2009

model presented by one author in [5], that concerns the inclusion of the iron(III)-hydroxide. In order to support the numerical results we have also built an experimental galvanic cell and obtained a good match of the experimental measurements and of the numerical results.

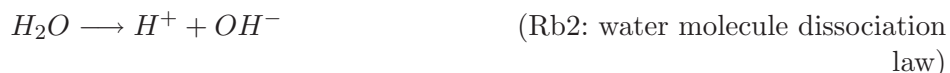
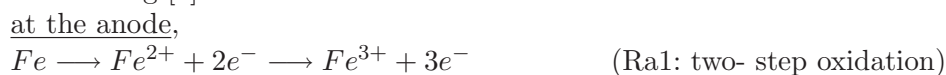
This paper is organized as follows: the next section details the experimental cell, in the third section the mathematical and numerical models are presented, finally, the fourth section is devoted to numerical and experimental results and their comparison.

2. Experimental Device.

We focus on the galvanic corrosion of an iron sample that may be represented as the oxidation process occurring in a galvanic cell where the iron sample plays the role of the anode.

The experimental galvanic cell that we have monitored in laboratory consists of an empty cylinder made of glass, closed at the two extrema by cylindrical electrodes: the anode, made of iron, and the cathode, made of platinum, a typical inert material. The two electrodes result 70 *cm* apart and their diameter is 5 *cm* long; the ratio between these quantities allows to assume the migration of the produced ions from one to the other electrode being negligible. Also the gravity effect is reduced by placing the cell on a horizontal plane. The electrodes are connected via a conducting wire outside of the cell where a potenziometer is placed in order to measure the electric potential gradient developed during the redox reactions.

It is known that main chemical reactions occurring in the galvanic cell are the following [7]:



being Fe^{2+} , the ferrous ion and Fe^{3+} , the ferric ion, OH^- , the hydroxyl ion, $Fe(OH)_3$, the iron (III)-hydroxide (rust precursor). In this work we present two tests, one with acidic electrolyte solution and one with neutral electrolyte solution.

3. Mathematical Model.

The geometrical shape of the described experimental cell is such that the unidimensional approximation is appropriate. Let us fix the origin of the reference frame at the anode and choose the x axis parallel to the symmetry axis of the cylindrical structure.

The chemical species involved in the process are: Fe^{3+} , H^+ , OH^- , $Fe(OH)_3$, A^- . Let $C_k = C_k(t, x)$, $k = 1, \dots, 5$, be their corresponding concentration (*moles/litre*) at time t and at abscissa x .

We have represented the reactions listed at the previous section by imposing, in the bulk, the mass conservation law, the condition of electro-neutrality of the system and the *rate law* of absorption/production of chemical species during a chemical reaction and by imposing, at the electrodes, the Butler-Volmer equation or the Hurd equation, where it applies, for the current density produced by redox reactions [6,7].

Neglecting the convective motion of the electrolyte, and under the assumption that concentrations are small, the mass flux \vec{J}_k of the k -th species is given, with a good approximation, by the Planck-Nernst law [7]:

$$(1) \quad \vec{J}_k = -D_k \nabla C_k - \frac{z_k F D_k}{RT} C_k \nabla \Phi$$

where D_k is the diffusion constant, z_k the charge number, F Faraday's constant, Φ the electric potential in the electrolyte, R the gas constant and T the absolute temperature. The law (1) represents the fact that the ions are transported by migration within the electric field and by molecular diffusion. For each species, by mass conservation, the following transport equation can be written in the electrolyte solution space:

$$(2) \quad \frac{\partial C_k}{\partial t} + \nabla \cdot \vec{J}_k = S_k$$

where S_k is a source term that takes into account the production (or absorption) of ions of the k -th species due to chemical reactions (*rate law*), as, for example, in the case of the ions Fe^{3+} that contribute to the formation of rust. For a binary reaction occurring between species i and j , on phenomenological basis, the *rate law* states:

$$S_k = \begin{cases} 0, & \text{if } k - th \text{ species is neither a produced} \\ & \text{nor a reacting species} \\ k_{ij}(C_i)^{\nu_i}(C_j)^{\nu_j}, & \text{if } k - th \text{ is a produced species} \\ \nu_k k_{ik}(C_i)^{\nu_i}(C_k)^{\nu_k}, & \text{if } k - th \text{ is a reacting species} \end{cases}$$

where k_{ij} , ν_i are the rate constant of the reaction between species $i - th$ and species $j - th$ (experimentally measured) and the stoichiometric coefficient of the $i - th$ species within the considered reaction, respectively.

It should be noticed that, once expression (1) is substituted in equation (2), this one takes the form of a convection-diffusion transport equation, where the transport velocity is proportional to $\nabla\Phi$. An equation for the electric potential Φ can be obtained considering the total electric current and imposing the electrical neutrality of the electrolyte. In fact the electrolyte is electrically neutral apart from the very thin double layers adjacent to the electrodes. The electric current density \vec{i} in the electrolyte is given in terms of the mass fluxes of ions by the Faraday's law:

$$(3) \quad \vec{i} = F \sum_k z_k \vec{J}_k.$$

A statement of electro-neutrality is that the electric current density is non-divergent, that is:

$$(4) \quad \nabla \cdot \vec{i} = 0.$$

Inserting expression (3) into equation (4) and taking into account the Planck-Nernst law (1), we obtain the equation for the electric potential:

$$(5) \quad \nabla \cdot \sum_k \frac{z_k^2 F D_k}{RT} C_k \nabla \Phi = - \sum_k z_k D_k \nabla^2 C_k.$$

Let us notice that when the concentration gradients are negligible, equation (5) reduces to the Laplace's equation, $\nabla^2 \Phi = 0$. Let us notice also that there is no advantage in solving the mass conservation equation for all the chemical species as the concentration of one ionic species can be derived just imposing local electro-neutrality and by solving a linear algebraic equation; we compute in this way the concentration of A^- that is C_5 :

$$(6) \quad 3C_1 + C_2 - C_3 = C_5.$$

3.1. Boundary Conditions.

At the anode and at the cathode, the redox reactions release respectively the following current densities:

$$(7) \quad i_a = z \frac{1 - \exp(-3F\eta/RT)}{\sum_{k=1}^2 \frac{n_k}{i_{0k}} \exp(-(z_{k-1} + \alpha_k n_k) \frac{F\eta}{RT})}$$

$$(8) \quad i_{c2} = i_{02} \exp\left((1 - \alpha) \frac{Fz_2}{RT} \eta_2\right)$$

$$i_{c3} = i_{03} \exp\left((1 - \alpha) \frac{Fz_3}{RT} \eta_3\right)$$

where

i_{0k} = exchange current density of the k – th reaction (experimental)

n_k = electron stoichiometric coefficient at the k – th step

α (and α_k) = transfer coefficient (experimental)

z_k = charge number of the k – th ion species

η = overvoltage produced by the anodic reactions,

being $\eta = \delta\Phi - E$, with $\delta\Phi$, the variation of potential between the electrode and the electrolyte (soon after the electronic double layer) and E is the electrode potential at zero current. The last quantity can be given as a function of the standard potential E^0 using the following Nernst equation:

$$E = E^0 + \frac{RT}{Fz} \sum_j \nu_j \ln(a_j),$$

where the summation is extended to all the species participating at the electrode reactions, ν_j are the stoichiometric coefficients and a_j are the activities of the ions. In the hypothesis of a diluted solution with a large excess of solvent, as we suppose in the present case, the activities of the ions can be approximated with the molar concentration C_j .

The overvoltages η_k , ($k = 2, 3$) attaining to the cathodic reactions, are obtained by $\eta_k = \delta\Phi - E_k$, with

$$E_k = E_k^0 + \frac{RT}{Fz} \nu_k \log(C_k),$$

where we can derive the meaning of the symbols from the expression of E . The expression (7) is known as the Hurd equation for the two-step oxidation of iron and the expressions (8) are known as Butler-Volmer equations (above, the current density released by H^+ reduction (reaction Rc1)

and, below, the current density released by OH^- formation (reaction Rc2). Then, boundary conditions are expressed in terms of the current density associated to each chemical species:

at the anode ($x = 0$), $Fz_1J_1 = i_a$, $J_2 = J_3 = J_4 = J_5 = 0$

at the cathode ($x = x_{max}$), $Fz_2J_2 = i_{c2}$ and $Fz_3J_3 = i_{c3}$, $J_1 = J_4 = J_5 = 0$.

In order to close the system two additional conditions are necessary, actually the electric potential is still undetermined. So we observe that, due to the electro-neutrality of the system, the current densities at the electrodes have to be equal:

$$Fz_1J_1(t, 0) = Fz_2J_2(t, x_{max}) + Fz_3J_3(t, x_{max}).$$

Moreover, after noting that the model depends just on the gradients of Φ , we are allowed to choose an arbitrary value for Φ at a point x of the domain.

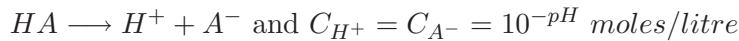
3.2. Initial Conditions.

The initial conditions are dependent only on the pH of the electrolytical solution. According to the well known dissociation law of the water molecule, we have:

$$-\log_{10}C_{H^+} - \log_{10}C_{OH^-} = 14;$$

and for pure water it is $pH = 7$, that is both ion concentrations equal 10^{-7} moles/litre.

When an acid is dissolved in water, it dissociates in ions according to the following formulas:



so the concentrations of H^+ ions increases and the pH of the solution decreases. Concerning the initial concentration $C_{OH^-} = 10^{-(14-pH)}$, it is considered negligible and not affecting, at initial time, the electro-neutrality of the solution. The initial concentrations of the other species ($k = 1, 4$) are assumed to be negligible.

3.3. Numerical Procedure.

The system of equations (2) and equations (5) and (6) is numerically solved by a finite difference discretization. The assignment of the discrete

unknowns on the mesh is staggered, with concentrations and electric potential in the middle of a cell and the fluxes \vec{J}_k at the extrema, in order to meet more easily and accurately the continuity equation. We have chosen second order time and space approximation schemes. In particular time integration has been accomplished by a predictor-corrector method based on the *mid-point* Euler scheme.

The natural characteristics of the problem announce the need of particular care in the numerical treatment of the unknowns and equations in the vicinity of the anode and cathode, where, actually, rapid increase and decrease of Φ occur. In these regions the process is transport dominated, whereas, in the centre of the cell, Φ is almost constant and, certainly, diffusion drives the evolution of the concentrations. We have faced the difficulties at the borders by using a stretched distribution of nodes towards the electrodes. A major specialization of the numerical scheme is beyond the scope of the present work that is aimed to verify the appropriateness of the mathematical model versus the application considered, iron corrosion within a galvanic cell set-up.

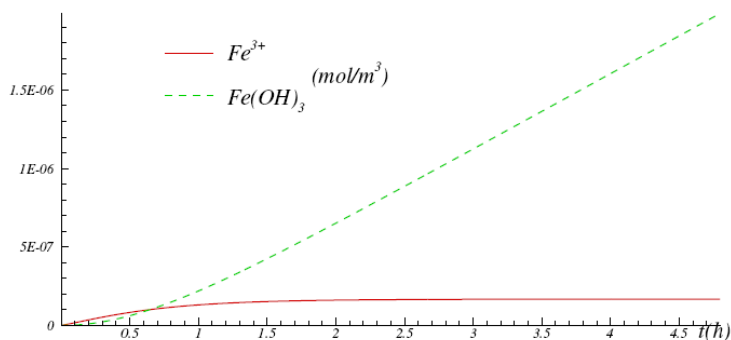


Fig. 1. Test-acidic: time evolution of the numerical concentrations in the neighbourhood of the anode.

4. Experimental and Numerical Test. Conclusion.

We have tested the mathematical model reproducing a galvanic cell filled with an acidic solution - the case that has most impact on industrial applications - and, as a further reliability check-up, we have solved also the case of neutral solution. The numerical solutions presented are obtained with space and time steps respectively $\Delta x = x_{max}/50$ and $\Delta t = 10^{-3}sec$,

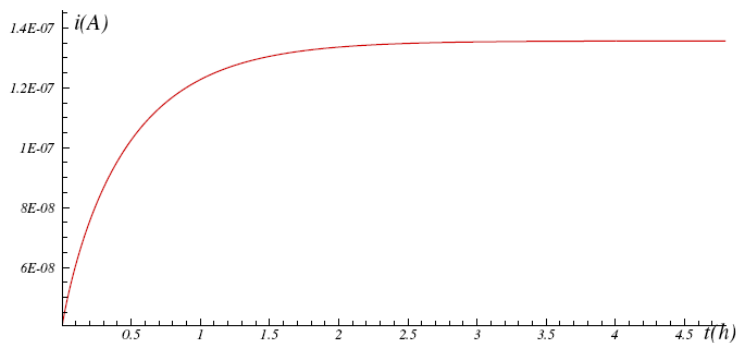


Fig. 2. Test-acidic: time evolution of the numerical current density released in the neighbourhood of the anode.

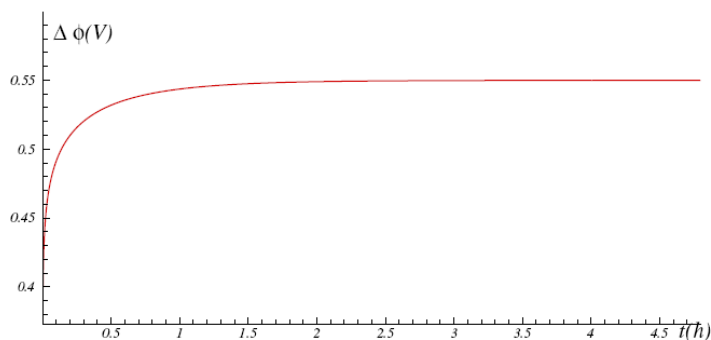


Fig. 3. Test-acidic: time evolution of the numerical electric potential gradient of the cell.

which have allowed a satisfactory matching with the measured quantities. For the values of the electrochemical constants appearing in the model we refer the reader to [8].

In the acidic case, the computed solution exhibits, for the concentrations of the Fe^{3+} ions and $Fe(OH)_3$ oxide at the first internal point aside the anode, the time evolution plotted in Figure 1. It is apparent that the ferric ion concentration increases asymptotically towards a value ($O(10^{-7})mole/m^3$), whereas, after the first hour, the iron(III)-oxide concentration grows at constant velocity: the anode loses continuously iron atoms and releases ferric ions and electrons and, after one hour adjustment, a constant portion of ferric ions contributes to the oxide formation. According to expectation, the time evolution of the current density (see plot in Figure 2) results reasonably similar to that one of the Fe^{3+} concentration, actually this one is proportional to the number of electrons released by the Fe atoms. Consequently it also holds that the more the concentration of $Fe(OH)_3$ oxide

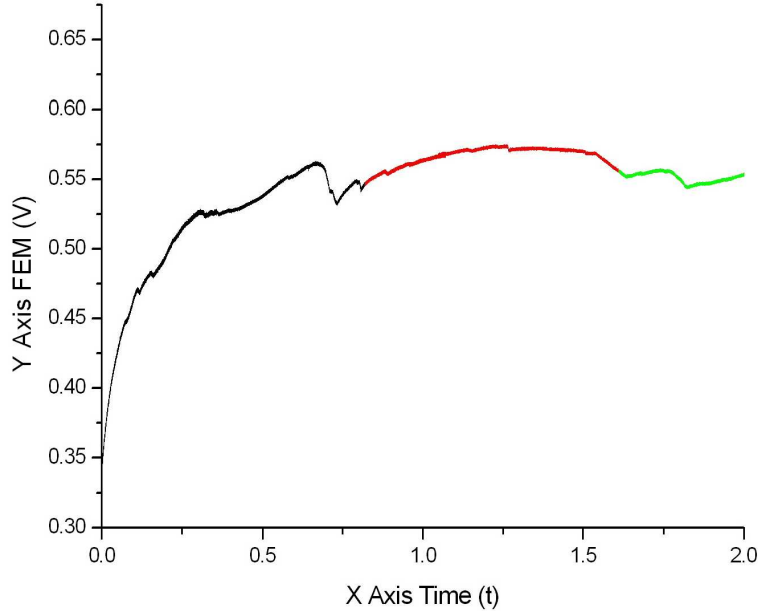


Fig. 4. Test-acidic: time evolution of the experimental electric potential gradient of the cell.

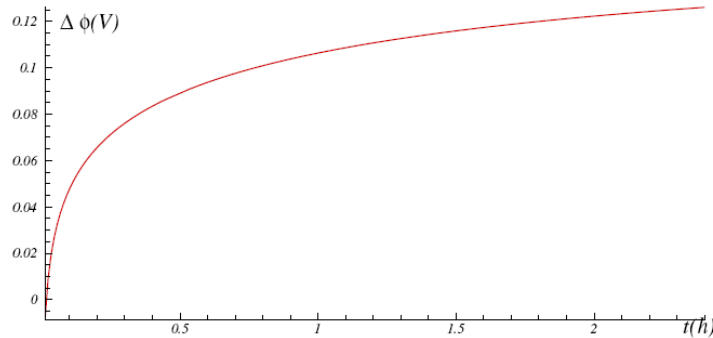


Fig. 5. Test-neutral: time evolution of the numerical electric potential gradient of the cell.

increases and the more the current density growth (that is its derivative) decreases. This behaviour may be referred as *passivation* [6], although this term is mainly used to indicate the effect of the layer of rust that forms on the anode and substantially prevents from new corrosion events to occur. The electric potential gradient developed during the simulated operation time of the galvanic cell (about $4.5h$) is drawn in Figure 3. We observe a very good qualitative matching with the experimental sketch in Figure 4, with respect to either the value and the passivation time (let us just notice that the experimental observation time interval is shorter and lasts $2h$).

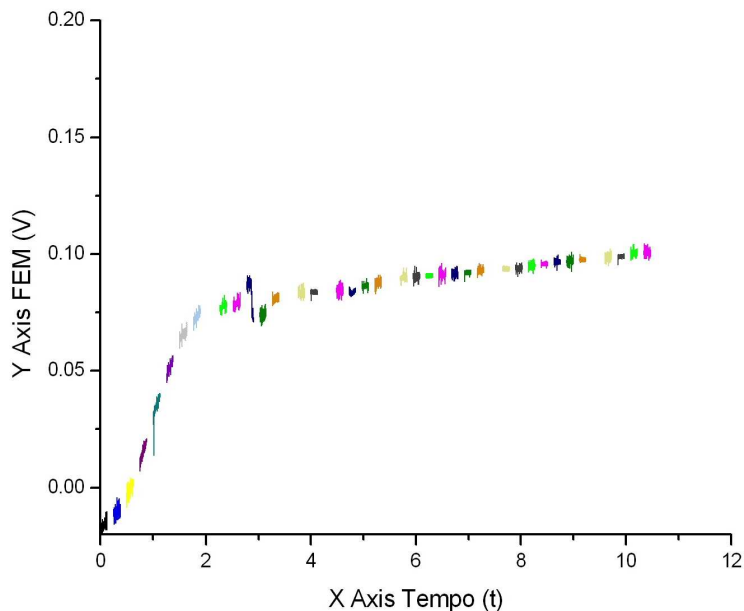


Fig. 6. Test-neutral: time evolution of the experimental electric potential gradient of the cell.

As further support to the mathematical and numerical model proposed, we display the curves of the numerical and experimental electric potential gradient for the case of neutral electrolytical solution, respectively in Figures 5 and 6. Also in this case we observe a substantial agreement. Moreover we observe that the value of Φ is considerably smaller than in the acidic case (actually, corrosion is less active in presence of a neutral solution) and the evolution towards passivation is slower (according to the overall behaviour). Next improvement of the mathematical model will be the inclusion of rust formation from the iron(III)-oxide and of the solutal convection with gravity effects. More care to the numerical procedure will be required in those cases. Our approach to the simulation of a galvanic cell will be much closer to the real process and will allow to recover exhaustively the passivation phenomenon, an important aspect for the implications on prevention treatments.

Acknowledgements.

Besides the institutional funding from C.N.R. in benefit of one author, we acknowledge the financial support of Soprintendenza ai Beni Culturali Regione Autonoma Valle d'Aosta (project "Analisi di processi di corrosione di materiali ferrosi", 2003-2005) that allowed to begin this research.

REFERENCES

1. T. A. Arias, J. Cline, A. A. Rigosand, Atomistic origins of corrosion : a fundamental ab initio view, *Physics and Materials Science, Gather/Scatter*, **13** (1997), pp. 2-35.
2. M. R. Radeke, E. A. Carter, Ab initio dynamics of surface chemistry, *Ann. Rev. Phys. Chem.*, **48** (1997), pp. 243-270.
3. G. Inglese, An inverse problem in corrosion detection, *Inverse problems*, **13** (1997), pp. 977 - 994.
4. G. Alessandrini, L. Del Piero, L. Rondi, Stable determination of corrosion by a single electrostatic boundary measurements, *Inverse problems*, **19** (2003), pp. 973 - 984.
5. V. Botte, D. Mansutti and A. Pascarelli, Numerical modeling of iron corrosion due to an acidic aqueous solution, *Applied Numerical Mathematics*, **55** (2005), pp. 253 - 263.
6. L. Kiss, *Kinetics of electrochemical metal dissolution*, Elsevier, 1988.
7. J. S. Newman, *Electrochemical systems*, Prentice-Hall, 1991.
8. R. Parson, *Handbook of electrochemical constants*, New York, Academic Press, 1959.